Monte Carlo Tuning with ATLAS Data

Frank Siegert
on behalf of the ATLAS collaboration
Albert-Ludwigs-Universität Freiburg

Table of Contents

What is Monte-Carlo tuning and why is it necessary?

Parameters in Monte-Carlo predictions

Perturbative parameters

- Particle properties
  masses, widths, …
- Factorisation/renormalisation scale
  process specific
- Running couplings
  some freedom – but consistent with PDF!
- Parton shower
  Evolution kernels

Are chosen/calculated, not tuned!

Non-perturbative parameters

- Multiple Parton Interactions (MPI)
  Infrared cut-off, energy evolution, …
- Hadronisation and hadron decays
  String vs. Cluster, BRs, form factors
- Primordial $k_\perp$
  $k_\perp$ distribution for incoming partons
- Parton shower
  Infrared cut-off

Unknown $\Rightarrow$ Need tuning to data.

Examples of relevant measurements

MPI	Underlying Event (UE) measurements at Tevatron and LHC
Hadronisation	LEP data on event shapes, identified hadrons, …
Primordial $k_\perp$	$p_\perp^{\ell\ell}$ in Drell-Yan events

How to compare to published measurements: Rivet

Features of the Rivet toolkit

- Generator independent implementation of analyses
- Event input through HepMC standard

⇒ Proper particle level definition of measurement crucial
(unfolded from detector effects, not "Z in event record", ...)

Available analyses

$>$ **100 experimental publications have been implemented in Rivet.**

- 15 from the LHC already (from all 4 experiments)
- Full spectrum from Tevatron:
  Distributions in W/Z, prompt photons, jets, UE, MinBias ... starting in 1988!
- LEP data from ALEPH, DELPHI, OPAL
- Only a few from HERA ($\rightarrow$ HZTool)

Tuning using Professor

Basic question

What is the most efficient way of scanning the n-dimensional parameter space of a MC generator to find the point with minimal χ^2 vs. data?

Procedure

1. Randomly sample N parameter points in n-dimensional space
2. Perform N generator runs and fill observables (e.g. with Rivet)
3. For each bin of each observable: Interpolate generator response in nD by fitting 3rd order polynomial
4. Minimise $\chi^2 = \sum_{\text{bins}} \frac{(\text{interpolation} - \text{data})^2}{\text{error}^2}$

$\Rightarrow$ Parameter values with expected best fit

The ATLAS detector

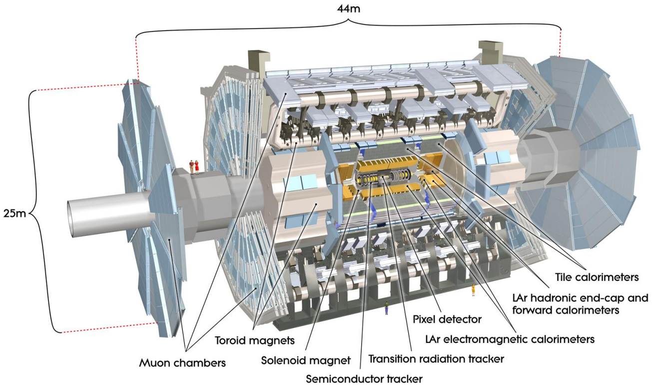

- Multi-purpose detector with three layers: Inner detector (tracking), calorimeters, muon spectrometer
- Additionally, Minimum Bias Trigger Scintillators were used in low-lumi runs to provide MB trigger

ATLAS Minimum Bias measurements

arXiv:1012.5104 [hep-ex]

- Charged particle distributions: $\frac{\mathrm{d}N}{\mathrm{d}p_\perp}, \frac{\mathrm{d}N}{\mathrm{d}N_\mathrm{ch}}, \frac{\mathrm{d}N}{\mathrm{d}\eta}, \langle p_\perp \rangle$ vs. N_ch
- $\sqrt{s} = 0.9, 2.36$ and 7 TeV
- Different event selection cuts: $N_\mathrm{ch} \geq 1,\ 2,\ 6,\ 20$
- Different particle selection cuts: $p_\perp > 100,\ 500$ MeV

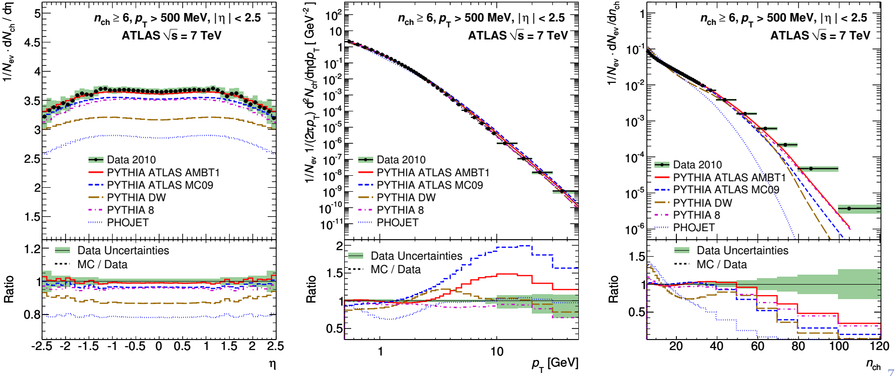

ATLAS Underlying Event measurements

arXiv:1012.0791 [hep-ex] and arXiv:1103.1816 [hep-ex]

- Both select leading object (track/cluster) with $p_\perp > 1$ GeV, $|\eta| \leq 2.5$
- Focus on activity in transverse region: $60° < |\Delta\phi = \phi - \phi_{\mathrm{lead}}| < 120°$ (most sensitive to UE)
- Activity = charged particles (tracks, 1012.0791) or charged+neutral particles (calorimeter clusters, 1103.1816)

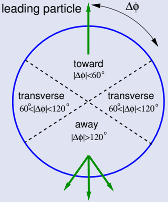

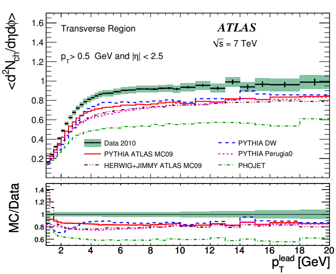

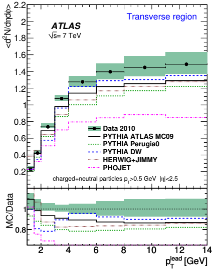

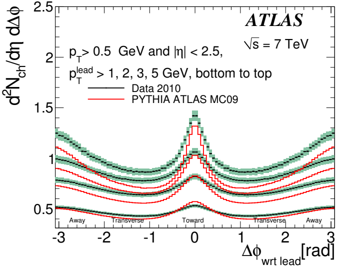

Jet measurements

Phys. Rev. D 83, 052003 (2011) [arXiv:1101.0070]

- Jet shapes in inclusive jet production
- Sensitive to initial state radiation
- Especially useful in Pythia tuning: FSR, ISR and "IFSR"

ATLAS-CONF-2010-049

- Fragmentation function of track jets
- Also sensitive to ISR
- Small tension of Pythia shower between fragmentation function and jet shapes

arXiv:1102.2696 [hep-ex]

- Dijet azimuthal decorrelations
- Also sensitive to ISR

arXiv:1012.5382 [hep-ex]

- W+jets measurements of leading jet $p_\perp$ in electron and muon channel

Overview

Herwig+Jimmy: AUET2 tunes

- Relatively simple tuning, only 3 parameters (Jimmy MPI)
- No soft inclusive QCD modelled $\Rightarrow$ Ignore MinBias
- Tunes for 10 PDFs using $\approx$ 50 CDF and ATLAS observables

Pythia6: AMBT2 and AUET2 tunes

- Existing tune (AMBT1 for LO* PDF) with focus on MinBias data
  $\Rightarrow$ Not optimal performance for UE observables and jet shapes
- New tune uses MRST LO** PDF
- Much more involved than Herwig+Jimmy:
  - 25 parameters (Hadronisation, ISR, MPI, primordial $k_\perp, \ldots$)
  - Hundreds of observables (LEP, Tevatron, ATLAS)

  $\Rightarrow$ 4 steps:
  1. Hadronisation flavour parameters (9) vs. LEP/SLD data
  2. FSR and hadronisation kinematics parameters (6) vs. LEP data
  3. ISR parameters (5) vs. jet data from Tevatron and ATLAS
  4. MPI parameters (5) vs. MinBias and UE data from Tevatron and ATLAS

Herwig+Jimmy: AUET2 tunes

Tuned parameters

Only three MPI parameters:

- Proton radius PRRAD
- Cut-off of QCD 2→2 scatterings in MPI and its energy dependence:

$$\texttt{PTJIM}(\sqrt{s}) = \texttt{PTJIM0} \left(\frac{\sqrt{s}}{1800\,\text{GeV}} \right)^{\texttt{EXP}}$$

Features

- Tunes for 10 PDF sets:
  MRSTMCal (LO**), CT09MC2, CTEQ6l1, MSTW08LO, CTEQ6.6, CT10, MSTW08NLO, HERAPDF1.0, HERAdis, NNPDF2.1
- Hard scattering required in model
  ⇒ MinBias data ignored
  ⇒ Soft parts of UE observables excluded from fits

Herwig+Jimmy: AUET2 tunes

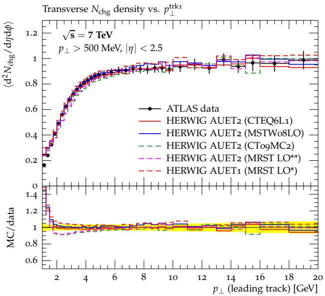

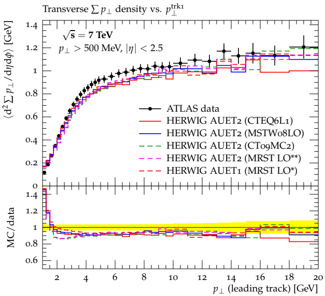

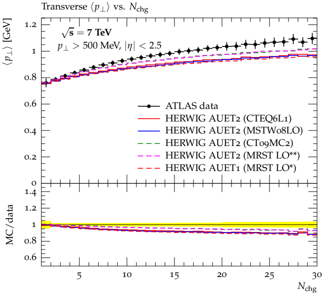

- LO and mLO PDFs here, similar picture for NLO PDFs
- Differences between PDFs can be "tuned away" for UE observables
- Slight tension between $\langle d^2 N_{ch} \rangle$ and $\langle d^2 \sum p_\perp \rangle$, in Pythia solved by colour reconnection
- Below MPI cut-off (≈ 5 GeV) soft physics modelling necessary

Herwig+Jimmy: AUET2 tunes

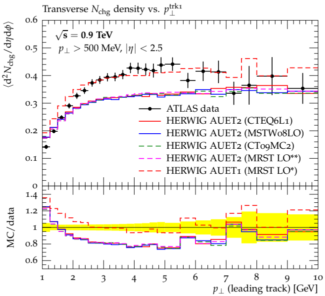

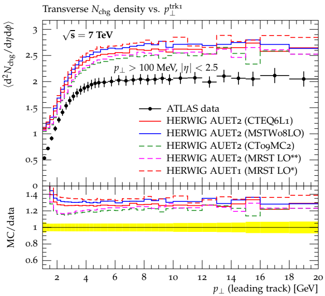

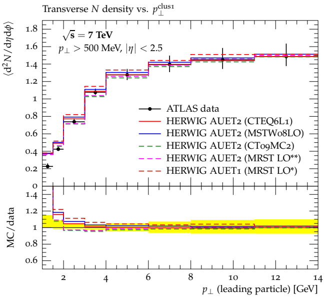

- Energy extrapolation model not sufficient to fit data at 630, 900 GeV, 2 TeV and 7 TeV simultaneously
- Not possible to fit ATLAS UE data with $p_\perp \geq 100$ MeV
- Nice fit also for cluster-based UE

Pythia6: AMBT2 and AUET2 tunes

Step 1: Hadronisation flavour parameters (9) vs. LEP/SLD data

- Flavour parameters tuned similarly as in [Buckley, Hoeth, Lacker, Schulz, v. Seggern: arXiv:0907.2973]

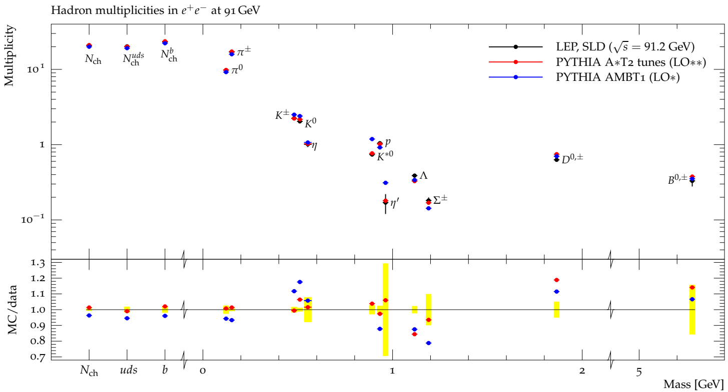

Pythia6: AMBT2 and AUET2 tunes

Step 2: FSR and hadronisation kinematics parameters (6) vs. LEP data

- In Pythia, FSR from resonance (Z/γ^*) decays is treated as distinct from ISR and FSR from partons produced in ISR
  $\Rightarrow$ Standalone tune of FSR and hadronisation kinematics to LEP data
- Again, similar as in arXiv:0907.2973 but with more input data
- Previous ATLAS tune (AMBT1) used Pythia's default parameters here, which are not optimal for $p_\perp$-ordered shower
- New tune (in red) does significantly better than AMBT1

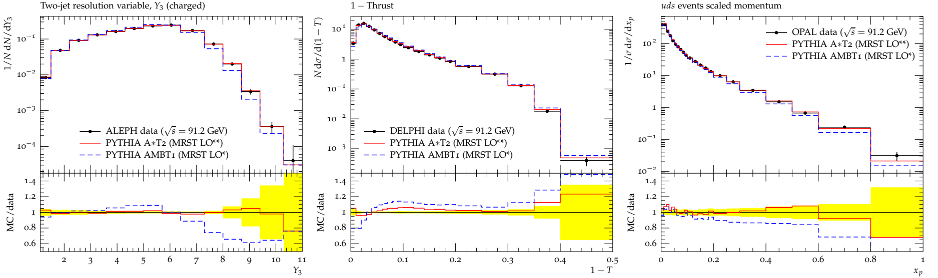

Pythia6: AMBT2 and AUET2 tunes

Step 3: ISR parameters (5) vs. jet data from Tevatron and ATLAS

- Jet shape measurements: AMBT1 jets too narrow
- Same problem in Perugia0 tune, fixed in Perugia2010 ⇒ New tune to follow Perugia2010 strategy for ISR
- Also includes primordial parton $k_\perp$ inside the hadron in tuning

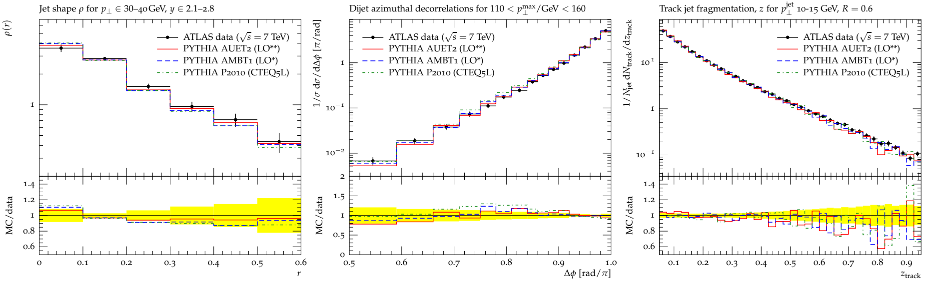

Pythia6: AMBT2 and AUET2 tunes

Step 4: MPI parameters (5) vs. MinBias and UE data

- MPI least theoretically constrained $\Rightarrow$ tuned last
- Not possible to find good tune (i.e. $< 20\%$ discrepancies) simultaneously for MB and UE data
  $\Rightarrow$ two separate tunes:
- AMBT2 for MinBias data
  - Improvements in statistically significant regions
  - $p_\perp$ distribution incompatibel with chosen ISR setup

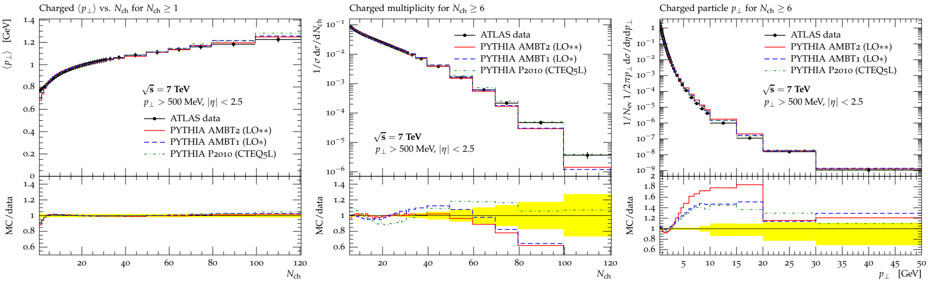

Pythia6: AMBT2 and AUET2 tunes

Step 4: MPI parameters (5) vs. MinBias and UE data

- MPI least theoretically constrained $\Rightarrow$ tuned last
- Not possible to find good tune (i.e. $< 20\%$ discrepancies) simultaneously for MB and UE data
  $\Rightarrow$ two separate tunes:
- AUET2 for UE data
  - Significant improvement over AMBT1 in plateau region
  - Also describes $p_\perp > 100$ MeV data well

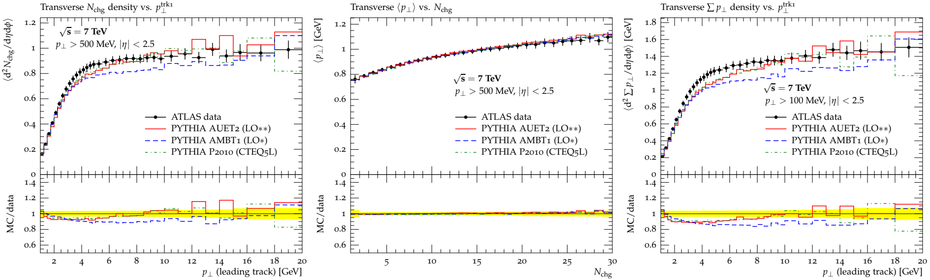

Conclusions

Summary

- Corrected ATLAS data are available for many MB, UE and jet observables
- It has been used for tuning Herwig+Jimmy and Pythia6

- Herwig+Jimmy has been tuned for several LO, mLO and NLO PDFs
- Limitations of the model have been demonstrated

- Pythia6 has been tuned for one PDF in all aspects: Hadronisation, FSR, ISR, MPI
- Significantly improved FSR and ISR tune
- MPI tune revealed limitations in describing MB and UE data simultaneously
  $\Rightarrow$ Separate tunes AMBT2 and AUET2

Outlook

- Probably last Herwig+Jimmy tune (due to model limitations)
  $\rightarrow$ future: Herwig++
- Incorporation of data from 2.76 TeV LHC run

Backup

Switches and fixed parameter values for Pythia6 tuning

Switch		A*T2
MSTP(52)	Use LHAPDF for external PDFs	2
MSTP(51)	Use MRST LO** PDF	20651
MSTJ(11)	Bowler-fragmentation function for heavy quarks	5
MSTJ(41)	$p_{\perp}$-ordered shower	12
MSTP(70)	ISR regularisation scheme with cut-off at PARP(62)/2	0
MSTP(64)	Set α_S scheme for ISR to CMW [b)]	3
MSTP(72)	Allow colour dipoles stretched between ISR dipoles to radiate FSR	2
MSTP(3)	Allow different α_S for different shower parts [a)]	1
MSTU(112)	Set number of flavours considered in α_S expression	4
PARU(112)	Set Λ in α_S running coupling calculation algorithm to Λ in PDF	0.265
PARP(1)	Set Λ_{QCD} in running α_S for hard scattering to Λ in PDF	0.265
PARP(61)	Set Λ_{QCD} in running α_S for ISR to Λ in PDF	0.265

a) Λ is given by PARP(1) for hard interactions, by PARP(61) for ISR, by PARP(72) for FSR not from a resonance decay, and by PARJ(81) for FSR from a resonance decay

b) This setting was introduced in PYTHIA6.419 and therefore undocumented in the PYTHIA6 manual. The release notes of PYTHIA6 refer to [1].

Observable-weight combinations for Pythia6 flavour tuning

Observable	Weight
OPAL measurements $Z \to q\bar{q}$, $\sqrt{s} = 91.2$ GeV [2]	
b quark frag. function $f(x_B^{\text{weak}})$	1
Mean of b quark frag. function $f(x_B^{\text{weak}})$	1
$u\,d\,s$ events mean charged multiplicity	1
c events mean charged multiplicity	1
b events mean charged multiplicity	1
All events mean charged multiplicity	1
LEP particle multiplicities ($\sqrt{s} = 91.2$ GeV), taken from PDG [3]	
$\pi^{\pm}$ multiplicity	1
π^{0} multiplicity	1
$\pi^{0}/\pi^{\pm}$ multiplicity ratio	6
$K^{+}/\pi^{\pm}$ multiplicity ratio	6
$K^{0}/\pi^{\pm}$ multiplicity ratio	6
$\eta/\pi^{\pm}$ multiplicity ratio	2
$\eta'(958)/\pi^{\pm}$ multiplicity ratio	1
$D^{+}/\pi^{\pm}$ multiplicity ratio	1
$D^{0}/\pi^{\pm}$ multiplicity ratio	1
$D_s^{+}/\pi^{\pm}$ multiplicity ratio	2
$(B^{+}, B_d^{0})/\pi^{\pm}$ multiplicity ratio	1
$B^{+}/\pi^{\pm}$ multiplicity ratio	1
$B_s^{0}/\pi^{\pm}$ multiplicity ratio	2
$\rho^{0}(770)/\pi^{\pm}$ multiplicity ratio	9
$\rho^{+}(770)/\pi^{\pm}$ multiplicity ratio	9
$\omega(782)/\pi^{\pm}$ multiplicity ratio	9
$K^{*+}(892)/\pi^{\pm}$ multiplicity ratio	2
$K^{*0}(892)/\pi^{\pm}$ multiplicity ratio	2
$\phi(1020)/\pi^{\pm}$ multiplicity ratio	1
$D^{*+}(2010)/\pi^{\pm}$ multiplicity ratio	1
$D_s^{*+}(2112)/\pi^{\pm}$ multiplicity ratio	1
$B^{*}/\pi^{\pm}$ multiplicity ratio	1
$p/\pi^{\pm}$ multiplicity ratio	3
$\Lambda/\pi^{\pm}$ multiplicity ratio	4
$\Sigma^{0}/\pi^{\pm}$ multiplicity ratio	2
$\Sigma^{\pm}/\pi^{\pm}$ multiplicity ratio	2
$\Xi^{-}/\pi^{\pm}$ multiplicity ratio	1
$\Delta^{++}(1232)/\pi^{\pm}$ multiplicity ratio	1
$\Sigma^{\pm}(1385)/\pi^{\pm}$ multiplicity ratio	1

Pythia6 flavour tuning results

Parameter i		i_{min}	i_{max}	A*T2	Default
PARJ(1)	Di-quark suppression	0.0	0.2	0.073	0.10
PARJ(2)	Strange suppression	0.1	0.4	0.2	0.30
PARJ(3)	Strange di-quark suppression	0.2	1.0	0.94	0.40
PARJ(4)	Spin-1 di-quark suppression	0.0	0.4	0.032	0.05
PARJ(11)	Spin-1 light meson	0.0	1.0	0.31	0.50
PARJ(12)	Spin-1 strange meson	0.0	1.0	0.4	0.60
PARJ(13)	Spin-1 heavy meson	0.0	1.0	0.54	0.75
PARJ(25)	η suppression	0.0	1.0	0.63	1.00
PARJ(26)	η' suppression	0.0	1.0	0.12	0.40

Observable-weight combinations for Pythia6 FSR/hadronisation tuning I

Observable	Fit range	Weight
Studies of QCD with the ALEPH detector. [4]		
Scaled momentum, $x_p = \|p\|/\|p_{\text{beam}}\|$ (charged)		1
Rapidity w.r.t. thrust axes, y_T (charged)	$x \leq 4$	1
Rapidity w.r.t. thrust axes, y_T (charged)	$4 \leq x \leq 6$	5
In-plane p_T in GeV w.r.t. sphericity axes (charged)		1
Out-of-plane p_T in GeV w.r.t. sphericity axes (charged)	$1 \leq x \leq 3.5$	1
Mean π^0 multiplicity		10
Jet rates and event shapes at LEP I and II [5]		
Thrust minor ($E_{\text{CMS}} = 91.2$ GeV)	$\ln T_{\text{minor}} \leq -4.0$	5
Thrust minor ($E_{\text{CMS}} = 91.2$ GeV)	$-4.0 \leq \ln T_{\text{minor}} \leq -0.5$	2
Jet mass difference ($E_{\text{CMS}} = 91.2$ GeV)		1
Aplanarity ($E_{\text{CMS}} = 91.2$ GeV)		1
Oblateness ($E_{\text{CMS}} = 91.2$ GeV)		1
Sphericity ($E_{\text{CMS}} = 91.2$ GeV)		1
Thrust ($E_{\text{CMS}} = 91.2$ GeV)		1
Heavy jet mass ($E_{\text{CMS}} = 91.2$ GeV)		1
Total jet broadening ($E_{\text{CMS}} = 91.2$ GeV)		1
Wide jet broadening ($E_{\text{CMS}} = 91.2$ GeV)		1
C-Parameter ($E_{\text{CMS}} = 91.2$ GeV)		1
Thrust major ($E_{\text{CMS}} = 91.2$ GeV)		1
Delphi MC tuning on event shapes and identified particles. [6]		
In-plane $p_\perp$ in GeV w.r.t. thrust axes	$0 \leq x \leq 8$	2
In-plane $p_\perp$ in GeV w.r.t. thrust axes	$8 \leq x \leq 14$	6
Out-of-plane $p_\perp$ in GeV w.r.t. thrust axes	$0 \leq x \leq 1$	2
Out-of-plane $p_\perp$ in GeV w.r.t. thrust axes	$1 \leq x \leq 10$	10
Rapidity w.r.t. thrust axes, y_T		2
Rapidity w.r.t. sphericity axes, y_S		2
Scaled momentum, $x_p = \|p\|/\|p_{\text{beam}}\|$		2
$1 -$ Thrust		1
Thrust major, M		1

Observable-weight combinations for Pythia6 FSR/hadronisation tuning II

Thrust minor, m		1
Oblateness = $M - m$		1
Sphericity, S		1
Aplanarity, A		1
Planarity, P		1
C parameter		1
D parameter		1
Heavy hemisphere masses, M_h^2 / E_{vis}^2		1
Light hemisphere masses, M_l^2 / E_{vis}^2		1
Difference in hemisphere masses, M_d^2 / E_{vis}^2		1
Wide hemisphere broadening, B_{max}		1
Narrow hemisphere broadening, B_{min}		1
Total hemisphere broadening, B_{sum}		1
Difference in hemisphere broadening, B_{diff}		1
Differential 3-jet rate with Durham algorithm, D_2^{Durham}		1
Differential 4-jet rate with Durham algorithm, D_3^{Durham}		1
Differential 5-jet rate with Durham algorithm, D_4^{Durham}		1
Energy-energy correlation, EEC		1
Asymmetry of the energy-energy correlation, AEEC		1
Mean charged multiplicity		5000
Study of the b-quark fragmentation function at LEP 1 [7]		
b quark fragmentation function $f(x_B^{\text{weak}})$	$0.25 \leq x \leq 1.0$	10
Mean of b quark fragmentation function $f(x_B^{\text{weak}})$		5
Jet rates in e^+e^- at JADE [35–44 GeV] and OPAL [91–189 GeV]. [8]		
Integrated 2-jet rate with Durham algorithm (91.2 GeV)		4
Integrated 3-jet rate with Durham algorithm (91.2 GeV)		4
Integrated 4-jet rate with Durham algorithm (91.2 GeV)		4
Integrated 5-jet rate with Durham algorithm (91.2 GeV)		4
Integrated $\geq$6-jet rate with Durham algorithm (91.2 GeV)		4
Differential 2-jet rate with Durham algorithm (91.2 GeV)		4
Differential 3-jet rate with Durham algorithm (91.2 GeV)		4

Observable-weight combinations for Pythia6 FSR/hadronisation tuning III

Differential 4-jet rate with Durham algorithm (91.2 GeV)	4
Differential 5-jet rate with Durham algorithm (91.2 GeV)	4
Measurements of flavor dependent fragmentation functions in $Z^0 -> q\bar{q}$ events [2]	
uds events scaled momentum	10
uds events mean charged multiplicity	500
Hadron multiplicities in hadronic e^+e^- events [3]	
Mean π^+ multiplicity	500
Mean π^0 multiplicity	500

Pythia6 FSR/hadronisation tuning results

Parameter i		i_{min}	i_{max}	A*T2	Default
`PARJ(21)`	σ_{string}	0.20	0.45	0.30	0.36
`PARJ(41)`	Lund_a	0.1	1.8	0.368	0.30
`PARJ(42)`	Lund_b	0.2	2.5	1.004	0.58
`PARJ(47)`	Bowler-fragmentation (for heavy quarks)	0.0	1.5	0.873	1.00
`PARJ(81)`	Λ_{QCD}	0.18	0.32	0.256	0.29
`PARJ(82)`	Shower cut-off	0.4	2.0	0.830	1.00

Observable-weight combinations for Pythia6 ISR/kT tuning

Observable	$\sqrt{s}$	Fit range	Weight
ATLAS jet shapes [9]			
Diff. jet shapes [a] ρ for $p_\perp \in [30, 40]$ GeV	7 TeV		1
Diff. jet shapes [a] ρ for $p_\perp \in [40, 60]$ GeV	7 TeV		1
Diff. jet shapes [a] ρ for $p_\perp \in [60, 80]$ GeV	7 TeV		1
Diff. jet shapes [a] ρ for $p_\perp \in [80, 110]$ GeV	7 TeV		1
Diff. jet shapes [a] ρ for $p_\perp \in [110, 160]$ GeV	7 TeV		1
Diff. jet shapes [a] ρ for $p_\perp \in [160, 210]$ GeV	7 TeV		1
Diff. jet shapes [a] ρ for $p_\perp \in [210, 260]$ GeV	7 TeV		1
Diff. jet shapes [a] ρ for $p_\perp \in [260, 310]$ GeV	7 TeV		1
Diff. jet shapes [a] ρ for $p_\perp \in [310, 400]$ GeV	7 TeV		1
Diff. jet shape ρ for $p_\perp \in [400, 500]$ GeV, $y \in [0.0, 2.8]$	7 TeV		5
Diff. jet shape ρ for $p_\perp \in [500, 600]$ GeV, $y \in [0.0, 2.8]$	7 TeV		5
ATLAS dijet decorrelations [10]			
$\Delta\phi_{12}, 110 < p_\perp^{\max} < 160$ GeV	7 TeV		5
$\Delta\phi_{12}, 160 < p_\perp^{\max} < 210$ GeV	7 TeV		5
$\Delta\phi_{12}, 210 < p_\perp^{\max} < 310$ GeV	7 TeV	$2.1 \leq \Delta\phi_{12} \leq \pi$	5
$\Delta\phi_{12}, p_\perp^{\max} < 310$ GeV	7 TeV	$2.3 \leq \Delta\phi_{12} \leq \pi$	5
ATLAS track jets [11]			
Longit. jet frag. function, z for $p_\perp^{\text{jet}} \in [4, 6]$ GeV, $R = 0.4$	7 TeV		5
Longit. jet frag. function, z for $p_\perp^{\text{jet}} \in [6, 10]$ GeV, $R = 0.4$	7 TeV		5
Longit. jet frag. function, z for $p_\perp^{\text{jet}} \in [10, 15]$ GeV, $R = 0.4$	7 TeV		5
Longit. jet frag. function, z for $p_\perp^{\text{jet}} \in [15, 24]$ GeV, $R = 0.4$	7 TeV		5
ATLAS W plus jets [13]			
1^{st} jet $p_\perp$ (electron channel)	7 TeV	$p_\perp > 40$ GeV	5
1^{st} jet $p_\perp$ (muon channel)	7 TeV	$p_\perp > 40$ GeV	5
CDF Z^0 $p_\perp$ and total cross-section in $Z \to e^+e^-$ [14]			
$p_\perp(Z^0)$	1800 GeV	$p_\perp < 10$ GeV	6
CDF jet shapes [15]			
Differential jet shapes [b] $\rho(r/R)$	1960 GeV		1
D0 dijet ϕ decorrelations [16]			
$\Delta\phi_{12}, p_\perp^{\max} \in [75, 100]$ GeV	1960 GeV		2
$\Delta\phi_{12}, p_\perp^{\max} \in [100, 130]$ GeV	1960 GeV		2
$\Delta\phi_{12}, p_\perp^{\max} \in [130, 180]$ GeV	1960 GeV		2
$\Delta\phi_{12}, p_\perp^{\max} > 180$ GeV	1960 GeV		2

[a] This observable enters the fit for five different, non-overlapping rapidity windows with the same weight: $y \in [0.0, 0.3], [0.3, 0.8], [0.8, 1.2], [1.2, 2.1], [2.1, 2.8]$

[b] A total of 18 ρ distributions with different, non-overlapping windows for the jet-$p_\perp$ from 37 to 380 GeV entered the fit. All had the same weight assigned.

Pythia6 ISR/kT tuning results

Description	PYTHIA Parameter	Tuning range	optimised value	AMBT1	Perugia 2010
ISR cut-off	PARP(62)	1.75–3.0	2.80	1.025	1.0
ISR scale factor on α_S eval. scale	PARP(64)	1.0–2.5	2.21	1.0	1.0
Scaling of max. parton virtuality	PARP(67)	0.1–2.0	0.66	4.0	1.0
Λ_{QCD} for FSR off ISR	PARP(72)	0.1–0.4	0.25	0.192	0.26
Primordial k_T	PARP(92)	0.8–2.5	1.92	2.0	2.0

Observable	$\sqrt{s}$	Weight
Track-based minimum bias at 900 GeV and 7 TeV in ATLAS [17]		
N_{ch}, track $p_\perp > 2500$ MeV, $N_{ch} \geq 1$	7 TeV	20
$p_\perp$, track $p_\perp > 2500$ MeV, $N_{ch} \geq 1$	7 TeV	20
η, track $p_\perp > 2500$ MeV, $N_{ch} \geq 1$	7 TeV	20
$\langle p_\perp \rangle$ vs. N_{ch}, track $p_\perp > 2500$ MeV, $N_{ch} \geq 1$	7 TeV	20
N_{ch}, track $p_\perp > 500$ MeV, $N_{ch} \geq 6$	7 TeV	40
$p_\perp$, track $p_\perp > 500$ MeV, $N_{ch} \geq 6$	7 TeV	40
η, track $p_\perp > 500$ MeV, $N_{ch} \geq 6$	7 TeV	40
$\langle p_\perp \rangle$ vs. N_{ch}, track $p_\perp > 500$ MeV, $N_{ch} \geq 6$	7 TeV	30
N_{ch}, track $p_\perp > 100$ MeV, $N_{ch} \geq 20$	7 TeV	10
$p_\perp$, track $p_\perp > 100$ MeV, $N_{ch} \geq 20$	7 TeV	10
η, track $p_\perp > 100$ MeV, $N_{ch} \geq 20$	7 TeV	10
$\langle p_\perp \rangle$ vs. N_{ch}, track $p_\perp > 100$ MeV, $N_{ch} \geq 20$	7 TeV	10
N_{ch}, track $p_\perp > 2500$ MeV, $N_{ch} \geq 1$	900 GeV	10
$p_\perp$, track $p_\perp > 2500$ MeV, $N_{ch} \geq 1$	900 GeV	10
η, track $p_\perp > 2500$ MeV, $N_{ch} \geq 1$	900 GeV	10
$\langle p_\perp \rangle$ vs. N_{ch}, track $p_\perp > 2500$ MeV, $N_{ch} \geq 1$	900 GeV	10
N_{ch}, track $p_\perp > 500$ MeV, $N_{ch} \geq 6$	900 GeV	20
$p_\perp$, track $p_\perp > 500$ MeV, $N_{ch} \geq 6$	900 GeV	20
η, track $p_\perp > 500$ MeV, $N_{ch} \geq 6$	900 GeV	20
$\langle p_\perp \rangle$ vs. N_{ch}, track $p_\perp > 500$ MeV, $N_{ch} \geq 6$	900 GeV	15
N_{ch}, track $p_\perp > 100$ MeV, $N_{ch} \geq 20$	900 GeV	5
$p_\perp$, track $p_\perp > 100$ MeV, $N_{ch} \geq 20$	900 GeV	5
η, track $p_\perp > 100$ MeV, $N_{ch} \geq 20$	900 GeV	5
$\langle p_\perp \rangle$ vs. N_{ch}, track $p_\perp > 100$ MeV, $N_{ch} \geq 20$	900 GeV	5
CDF Run II minimum bias [18]		
$\langle p_\perp \rangle$ vs. N_{ch}	1960 GeV	5

Table: Observable–weight combinations used for the AMBT2 MPI tuning.

Observable-weight combinations for Pythia6 MPI tuning (UE) I

Observable	$\sqrt{s}$	Fit range	Weight
Track-based underlying event at 900 GeV and 7 TeV in ATLAS [19]			
Transverse region N_{chg} density vs. $p_\perp$ (leading track)	7 TeV	$\geq$ 6 GeV	40
Toward region N_{chg} density vs. $p_\perp$ (leading track)	7 TeV	$\geq$ 6 GeV	10
Away region N_{chg} density vs. $p_\perp$ (leading track)	7 TeV	$\geq$ 6 GeV	10
Transverse region $\sum p_\perp$ density vs. $p_\perp$ (leading track)	7 TeV	$\geq$ 6 GeV	40
Toward region $\sum p_\perp$ density vs. $p_\perp$ (leading track)	7 TeV	$\geq$ 6 GeV	10
Away region $\sum p_\perp$ density vs. $p_\perp$ (leading track)	7 TeV	$\geq$ 6 GeV	10
Transverse region $\langle p_\perp \rangle$ density vs. $p_\perp$ (leading track)	7 TeV		40
Toward region $\langle p_\perp \rangle$ density vs. $p_\perp$ (leading track)	7 TeV		10
Away region $\langle p_\perp \rangle$ density vs. $p_\perp$ (leading track)	7 TeV		10
Transverse region $\langle p_\perp \rangle$ density vs. N_{ch} (leading track)	7 TeV		40
Toward region $\langle p_\perp \rangle$ density vs. N_{ch} (leading track)	7 TeV		10
Away region $\langle p_\perp \rangle$ density vs. N_{ch} (leading track)	7 TeV		10
Transverse region N_{chg} density vs. $p_\perp$ (leading track), $p_\perp > 100$ MeV	7 TeV		10
Toward region N_{chg} density vs. $p_\perp$ (leading track), $p_\perp > 100$ MeV	7 TeV		4
Away region N_{chg} density vs. $p_\perp$ (leading track), $p_\perp > 100$ MeV	7 TeV		4
Transverse region $\sum p_\perp$ density vs. $p_\perp$ (leading track), $p_\perp > 100$ MeV	7 TeV		10
Toward region $\sum p_\perp$ density vs. $p_\perp$ (leading track), $p_\perp > 100$ MeV	7 TeV		4
Away region $\sum p_\perp$ density vs. $p_\perp$ (leading track), $p_\perp > 100$ MeV	7 TeV		4
Transverse region N_{chg} density vs. $p_\perp$ (leading track)	900 GeV	$\geq$ 3 GeV	20
Toward region N_{chg} density vs. $p_\perp$ (leading track)	900 GeV	$\geq$ 3 GeV	5
Away region N_{chg} density vs. $p_\perp$ (leading track)	900 GeV	$\geq$ 3 GeV	5
Transverse region $\sum p_\perp$ density vs. $p_\perp$ (leading track)	900 GeV	$\geq$ 3 GeV	20
Toward region $\sum p_\perp$ density vs. $p_\perp$ (leading track)	900 GeV	$\geq$ 3 GeV	5
Away region $\sum p_\perp$ density vs. $p_\perp$ (leading track)	900 GeV	$\geq$ 3 GeV	5
Transverse region $\langle p_\perp \rangle$ density vs. $p_\perp$ (leading track)	900 GeV		20
Toward region $\langle p_\perp \rangle$ density vs. $p_\perp$ (leading track)	900 GeV		5
Away region $\langle p_\perp \rangle$ density vs. $p_\perp$ (leading track)	900 GeV		5
Transverse region $\langle p_\perp \rangle$ density vs. N_{ch} (leading track)	900 GeV		20

Toward region $\langle p_\perp \rangle$ density vs. N_{ch} (leading track)	900 GeV		5
Away region $\langle p_\perp \rangle$ density vs. N_{ch} (leading track)	900 GeV		5
Transverse region N_{chg} density vs. $p_\perp$ (leading track), $p_\perp > 100$ MeV	900 GeV		5
Toward region N_{chg} density vs. $p_\perp$ (leading track), $p_\perp > 100$ MeV	900 GeV		2
Away region N_{chg} density vs. $p_\perp$ (leading track), $p_\perp > 100$ MeV	900 GeV		2
Transverse region $\sum p_\perp$ density vs. $p_\perp$ (leading track), $p_\perp > 100$ MeV	900 GeV		5
Toward region $\sum p_\perp$ density vs. $p_\perp$ (leading track), $p_\perp > 100$ MeV	900 GeV		2
Away region $\sum p_\perp$ density vs. $p_\perp$ (leading track), $p_\perp > 100$ MeV	900 GeV		2
Cluster-based underlying event at 900 GeV and 7 TeV in ATLAS [20]			
Transverse N density vs. $p_\perp^{\text{clus1}}$	7 TeV		20
Transverse $\sum p_\perp$ density vs. $p_\perp^{\text{clus1}}$	7 TeV		20
Transverse N density vs. $p_\perp^{\text{clus1}}$	900 GeV		10
Transverse $\sum p_\perp$ density vs. $p_\perp^{\text{clus1}}$	900 GeV		10
Field & Stuart Run I underlying event analysis [21]			
N_{ch} (toward) for min-bias	1800 GeV	$\geq$ 4 GeV	3
N_{ch} (transverse) for min-bias	1800 GeV	$\geq$ 4 GeV	5
N_{ch} (away) for min-bias	1800 GeV	$\geq$ 4 GeV	3
N_{ch} (toward) for JET20	1800 GeV		3
N_{ch} (transverse) for JET20	1800 GeV		5
N_{ch} (away) for JET20	1800 GeV		3
$p_\perp^{\text{sum}}$ (toward) for min-bias	1800 GeV	$\geq$ 4 GeV	3
$p_\perp^{\text{sum}}$ (transverse) for min-bias	1800 GeV	$\geq$ 4 GeV	5
$p_\perp^{\text{sum}}$ (away) for min-bias	1800 GeV	$\geq$ 4 GeV	3
$p_\perp^{\text{sum}}$ (toward) for JET20	1800 GeV		3
$p_\perp^{\text{sum}}$ (transverse) for JET20	1800 GeV		5
$p_\perp^{\text{sum}}$ (away) for JET20	1800 GeV		3
$p_\perp$ distribution (transverse, $p_\perp^{\text{lead}} > 5$ GeV)	1800 GeV		3
$p_\perp$ distribution (transverse, $p_\perp^{\text{lead}} > 30$GeV)	1800 GeV		3
Transverse cone and 'Swiss cheese' underlying event studies [22]			

Observable-weight combinations for Pythia6 MPI tuning (UE) III

Transverse cone $\langle p_\perp^{\text{max}} \rangle$ vs. $E_\perp^{\text{lead}}$	1800 GeV	5
Transverse cone N_{max} vs. $E_\perp^{\text{lead}}$	1800 GeV	5
Swiss Cheese $p_\perp^{\text{sum}}$ vs. $E_\perp^{\text{lead}}$ (2 jets removed)	1800 GeV	5
Swiss Cheese $p_\perp^{\text{sum}}$ vs. $E_\perp^{\text{lead}}$ (3 jets removed)	1800 GeV	5
Transverse cone $\langle p_\perp^{\text{max}} \rangle$ vs. $E_\perp^{\text{lead}}$	630 GeV	5
Swiss Cheese $p_\perp^{\text{sum}}$ vs. $E_\perp^{\text{lead}}$ (2 jets removed)	630 GeV	5
Swiss Cheese $p_\perp^{\text{sum}}$ vs. $E_\perp^{\text{lead}}$ (3 jets removed)	630 GeV	5
CDF Run 2 underlying event in leading jet events [23]		
Transverse region charged particle density	1960 GeV	20
TransMAX region charged particle density	1960 GeV	10
TransMIN region charged particle density	1960 GeV	10
TransDIF region charged particle density	1960 GeV	2
Transverse region charged $\sum p_\perp$ density	1960 GeV	20
TransMAX region charged $\sum p_\perp$ density	1960 GeV	10
TransMIN region charged $\sum p_\perp$ density	1960 GeV	10
TransDIF region charged $\sum p_\perp$ density	1960 GeV	2
Transverse region charged $\langle p_\perp \rangle$ density	1960 GeV	10
CDF Run 2 underlying event in Drell-Yan [23]		
Toward region charged particle density	1960 GeV	20
Transverse region charged particle density	1960 GeV	10
TransMAX region charged particle density	1960 GeV	5
TransMIN region charged particle density	1960 GeV	5
Away region charged particle density	1960 GeV	5
Toward region charged $p_\perp^{\text{sum}}$ density	1960 GeV	20
Transverse region charged $p_\perp^{\text{sum}}$ density	1960 GeV	10
TransMAX region charged $p_\perp^{\text{sum}}$ density	1960 GeV	5
TransMIN region charged $p_\perp^{\text{sum}}$ density	1960 GeV	5
Away region charged $p_\perp^{\text{sum}}$ density	1960 GeV	5
Toward region charged $p_\perp^{\text{max}}$ density	1960 GeV	2
Transverse region charged $p_\perp^{\text{max}}$ density	1960 GeV	2

Away region charged $p_\perp^{\max}$ density	1960 GeV	2
Charged $\langle p_\perp^{\ell\ell} \rangle$ vs. N_{ch}	1960 GeV	10
Charged $\langle p_\perp \rangle$ vs. N_{ch}	1960 GeV	10
Charged $\langle p_\perp \rangle$ vs. N_{ch}, $p_\perp(Z^0) < 10$ GeV	1960 GeV	10

Pythia6 MPI tuning results

Description	PYTHIA Parameter	Tuning range	AMBT2	AUET2	AMBT1	Perugia 2010
Fast string CR	PARP(77)	0.25–1.15	0.88	1.12	1.02	1.00
CR strength	PARP(78)	0.1–0.6	0.18	0.33	0.54	0.35
$p_{\perp}^{0}$ ($\sqrt{s}$ = 1800 GeV)	PARP(82)	2.1–2.7	2.49	2.45	2.29	2.05
Matter distribution	PARP(84)	0.0–1.0	0.62	0.53	0.65	– a)
$p_{\perp}^{0}$ $\sqrt{s}$ evolution exponent	PARP(90)	0.18–0.28	0.244	0.229	0.250	0.26

a) Perugia 2010 uses a exponential matter distribution which doesn't use this parameter.

- S. Catani, B. R. Webber and G. Marchesini, Nucl. Phys. B **349** (1991) 635.
- K. Ackerstaff *et al.* [OPAL Collaboration], Eur. Phys. J. C **7** (1999) 369 [arXiv:hep-ex/9807004].
- C. Amsler *et al.* [Particle Data Group], Phys. Lett. B **667** (2008) 1.
- R. Barate *et al.* [ALEPH Collaboration], Phys. Rept. **294** (1998) 1.
- A. Heister *et al.* [ALEPH Collaboration], Eur. Phys. J. C **35** (2004) 457.
- P. Abreu *et al.* [DELPHI Collaboration], Z. Phys. C **73** (1996) 11.
- G. Barker *et al.* [DELPHI Collaboration], DELPHI-2002-069-CONF-603.
- P. Pfeifenschneider *et al.* [JADE collaboration and OPAL Collaboration], Eur. Phys. J. C **17** (2000) 19 [arXiv:hep-ex/0001055].
- G. Aad *et al.* [Atlas Collaboration], arXiv:1101.0070 [hep-ex].
- J. B. G. da Costa *et al.* [ATLAS Collaboration], arXiv:1102.2696 [hep-ex].
- S. Zenz [ATLAS Collaboration], ATL-PHYS-PROC-2010-135.
- G. Aad *et al.* [ATLAS Collaboration], ATLAS-CONF-2010-049.
- G. Aad *et al.* [ATLAS Collaboration], Phys. Lett. B **698** (2011) 325 [arXiv:1012.5382 [hep-ex]].

- A. A. Affolder *et al.* [CDF Collaboration], Phys. Rev. Lett. **84** (2000) 845 [arXiv:hep-ex/0001021].
- D. E. Acosta *et al.* [CDF Collaboration], Phys. Rev. D **71** (2005) 112002 [arXiv:hep-ex/0505013].
- V. M. Abazov *et al.* [D0 Collaboration], Phys. Rev. Lett. **94** (2005) 221801 [arXiv:hep-ex/0409040].
- G. Aad *et al.* [ATLAS Collaboration], arXiv:1012.5104 [hep-ex].
- T. Aaltonen *et al.* [CDF Collaboration], Phys. Rev. D **79** (2009) 112005 [Erratum-ibid. D **82** (2010) 119903] [arXiv:0904.1098 [hep-ex]].
- G. Aad *et al.* [Atlas Collaboration], arXiv:1012.0791 [hep-ex].
- G. Aad *et al.* [ATLAS Collaboration], arXiv:1103.1816 [hep-ex].
- A. A. Affolder *et al.* [CDF Collaboration], Phys. Rev. D **65** (2002) 092002.
- D. E. Acosta *et al.* [CDF Collaboration], Phys. Rev. D **70** (2004) 072002 [arXiv:hep-ex/0404004].
- T. Aaltonen *et al.* [The CDF Collaboration], Phys. Rev. D **82** (2010) 034001 [arXiv:1003.3146 [Unknown]].